EIGHT-DEGREES-OF-FREEDOM KINEMATIC MODEL DEMONSTRATING AFTER-IMPACT MOTORCYCLE'S BEHAVIOR

Tang-Hsien Chang
Department of Civil Engineering
National Taiwan University
Taipei, Taiwan 106, R.O.C.

Key Words: two-wheel vehicle dynamics, impacted motorcycle kinematics, accidental analytical tool.

ABSTRACT

Deriving a precise kinematic model to describe a motorcycle's behavior after impact is a prerequisite for developing a fact-analytical tool for motorcycle accidents. Therefore, this paper successfully derives a high-degrees-of-freedom model. Twenty-four time-response illustrations of simulation results demonstrate the dynamic behavior of the proposed model. A surface diagram is revealed while investigating the vehicle tracking. The twenty-four illustrations include motion, velocity and acceleration with respect to longitudinal, lateral, vertical, pitching, yawing, vehicle rolling, rider rolling, and steering variations. The model proposed herein can be effectively used to preliminarily analyze the tendency toward stability or toward rolling of a motorcycle after a collision.

I. INTRODUCTION

A two-wheel vehicle is a conventional transportation mode in developing countries. Taiwan has around nine million motorcycles, which is roughly half the total population. Unfortunately, according to official statistics, approximately two-thirds of all accidents are related to motorcycles. Thousands of people are injured and killed in motorcycle accidents annually. The actual causes of such accidents are frequently misunderstood owing to the lack of an accurate analytical tool. From a professional perspective, examining motorcycle accidents is still difficult owing to high degrees of freedom of motorcycle kinematics. Therefore, a reasonably accurate analytical tool must be developed to enhance the precision of investigation and examination. Although some developing software for accident reconstruction is available in Japan and the United States (Woolley *et al.*, 1986), only four-wheel cars are considered. Simulation or motorcycle accidents is much more complicated than passenger car accidents. Nevertheless, several institutes and professionals have offered promising results, including Danver Research Institute (Knight, and Peterson, 1971), Sporner (1982) and TRRL (Happian-Smith *et al.*, 1987; 1990). Recently, Lupker *et al.*, (1991, 1992) utilized MADYMO software to develop a motion analysis of motorcycle collisions and even calibrated it to apply to YAMAHA SRX-600 bikes (heavy model). However, those motorcycle-rider systems for accident analysis are still limited to some collision types. Most types of motorcycles in Taiwan and developing countries are light models, accounting for the need to modify kinematic models.

Although developing an analytical tool for motorcycle accidents is rather complicated owing to high degrees of freedom of motion in motorcycles, deriving a precise kinematic model to describe an impacted motorcycle's behavior is a relevant task. Therefore, in this paper, we derive a nonlinear systematic motorcycle-rider kinematic model to analyze the response of a motorcycle after an external force acts upon it. The proposed model is a prescription as well as a base for accident reconstruction when motorcycles are involved. The model proposed herein considers eight degrees of freedom of the motorcycle-rider system, including a vehicle's approaching, lateral, vertical, rolling, yawing, pitching, steering and rider's leaning variations. The input variables during a collision are initial velocities, volume, position and angle of acting forces. In addition, the trajectory of each component is investigated in a case study, in which the system variation with twenty-four variables is represented by time-dependent simulation. Simulation results demonstrate that the proposed model can easily trace the motion of an impacted motorcycle and obtain reasonable explanations for accidents.

II. KINEMATIC EQUATION

The structure of a motorcycle is simpler than that of a passenger car. However, motorcycles have more degrees of freedom with respect to maneuver and motion. Deriving rigorous dynamics for motorcycles is rather difficult. Most related investigations merely emphasize motion stability issues, accounting for why they only consider linearly lateral, rolling, yawing and steering dynamics based on an assumption of a constant speed (Sharp, 1971; Weir and Zellner, 1978; Katayama *et al.*, 1988; Yeh and Chen, 1990; Chang, 1992). Sharp (1971) derived equations of motion for motorcycle stability and control. Weir and Zellner (1978) utilized four degrees of freedom to analyze capsizing, weaving and wobbling modes of a motorcycle-rider system. Katayama *et al.* (1988) applied six degrees of freedom to describe a motorcycle-rider system. According to their results, the relationship of steering torque τ, roll angle ϕ and heading error d is $\tau = a'\phi + c'd'$, where $78 < a' < 103$ (Nm/rad), c' and d' are constants. Yeh and Chen (1990) and Chang (1992) analyzed the handling stability of a motorcycle with front cambering and a trailer, respectively. In addition, Rice (1978) investigated the relationship between a rider's lean angle and steering torque. Aoki (1979) indicated that the major motorcycle control input is steering torque. Liu and Chen (1992) investigated the nonlinear stability boundary with Legouis *et al.* (1986) and Weir's models (1972). TNO (1994) has recently developed MADYMO software capable of simulating motorcycle dynamics. In MADYMO, a rider's control torque is expressed as

$$\tau = -a\phi - b\dot{\phi} \tag{1}$$

According to TNO's experiment, a=15 and b=60 (1994). However, their models consider pitch and vertical motions to a lesser extent. Pitch and vertical motions should be included if a kinematic model is developed for accident analysis or safety evaluation of roadway facility design.

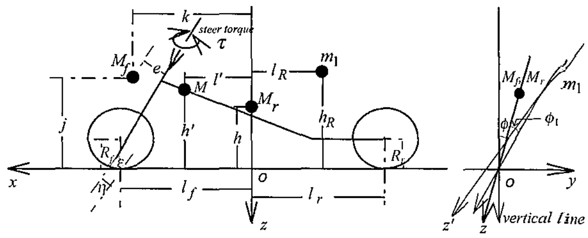

Fig. 1 A motorcycle-rider frame

1. Frame Coordinate System

In this study, the motorcycle-rider system is divided into three portions: front body, main body (rear body) and rider. The front body includes a front wheel, fork, and handle-bar. The bar can be rotated at an angle of δ. The main body includes an engine, gear-box, body frame and rear wheel. The model proposed herein considers the rider's leaning action. Fig. 1 depicts the mass centers of those three portions. The coordinate system for modeling is also included in this figure. Where the x-axis coincides with the traveling direction of the motorcycle, the y-axis is directive to the right (starboard), and the z-axis crosses though the main frame's center and is identical to gravity. The xy-surface is tangent to the earth. The three axes intersect at 'O' which is the origin of the motion system. The vehicle is assumed herein to be symmetrical to the xz-plane. In addition, the right-hand rule, i.e. 'clockwise rotation is positive', is applied in the mechanical analysis.

2. System Description

An eight-degrees-of-freedom model is constructed herein, which include a vehicle's approaching, lateral, vertical, rolling, yawing, pitching, steering and rider's leaning variation. An external force applied to the system is also included to investigate the motorcycle's motion behavior during impact.

The proposed model describes the kinematic behavior of a motorcycle-rider system when it encounters an external force. If the system, acted on by a force, is controllable by the rider, the system gradually recovers to stable conditions. Otherwise, if it is out of control, the system finally overturns. Several assumptions in this analysis are described as follows:

(i) The motorcycle is symmetrical to the xz-plane, and the rider is symmetrical to the $x'z'$ and the $y'z'$-planes. In addition, the x-y-z coordinate system is fixed on the motorcycle and the x'-y'-z' coordinate system is fixed on the rider;

(ii) The motorcycle is assumed to be moving on a flat road. This model neglects the effects of suspension, relaxation characteristics and aligning torque on tires. No slipping occurrence is considered with respect to tires;

(iii) The characteristics of the rider's body action are represented by body stiffness, in terms of a natural frequency, ω_1, and a damping ratio ζ_1 (Katayama *et al.*, 1988). The rider can apply a torque, τ, on the steering to handle the vehicle. The torque is a function of the rolling angle ϕ and the rolling velocity $\dot{\phi}$ (TNO, 1994);

(iv) After a collision occurs, braking, accelerating and mechanism damage as well as deformation, are not considered;

(v) Owing to the small projection of the motorcycle, air resistance is negligible. However, rolling resistance should be considered. In general, rolling resistance can be expressed as

$$F_r=\mu W \tag{2}$$

where μ denotes the coefficient of rolling resistance and W represents the total weight including vehicle and rider; and

(vi) The scanning time interval in later simulations is set to be sufficiently small to hold that $\sin\phi=\phi$, $\sin\phi_1=\phi_1$, $\sin\delta=\delta$ and $\sin\dot{\phi}_1 = \dot{\phi}_1$ etc.

3. Motorcycle-Rider System Dynamics

Based on the position vectors of the centers of mass of the front body, main body and rider corresponding to the earth, the relative translation motions with respect to velocity and acceleration can be derived. According to the x- and y- as well as z-components of the motion of acceleration, the forces of inertia related to longitudinal, lateral and vertical directions are represented as

$$\begin{aligned}\Sigma \boldsymbol{F}_x^i &= (M_f + M_r + m_1)\ddot{X} - (M_f + M_r + m_1)\dot{Y}\dot{\psi} \\ &- (M_f j + M_r h + m_1 h_R)\dot{\phi}\dot{\psi} - (m_1 h_R)\dot{\phi}_1\dot{\psi} \\ &- (M_f k - m_1 l_R)\dot{\psi}^2 - (M_f e\cos\varepsilon)\dot{\delta}^2 \\ &- (M_f j + M_r h + m_1 h_R)\ddot{\varphi} + (M_f + M_r + m_1)\dot{Z}\dot{\varphi} \\ &- (M_f k - m_1 l_R)\dot{\varphi}^2\end{aligned} \tag{3}$$

$$\begin{aligned}\Sigma \boldsymbol{F}_y^i &= (M_f + M_r + m_1)\ddot{Y} + (M_f j + M_r h + m_1 h_R)\ddot{\phi} \\ &+ (m_1 h_R)\ddot{\phi}_1 + (M_f k - m_1 l_R)\ddot{\psi} + (M_f e)\ddot{\delta} \\ &+ (M_f + M_r + m_1)\dot{X}\dot{\psi} - (M_f j + M_r h \\ &+ m_1 h_R)\varphi\dot{\psi} - (M_f + M_r + m_1)\dot{Z}\dot{\phi} - (m_1)\dot{Z}\dot{\phi}_1 \\ &+ (M_f k - m_1 l_R)\dot{\phi}\dot{\varphi} - (m_1 l_R)\dot{\phi}_1\dot{\varphi}\end{aligned} \tag{4}$$

$$\begin{aligned}\Sigma \boldsymbol{F}_z^i &= (M_f + M_r + m_1)\ddot{Z} + (M_f + M_r + m_1)\dot{Y}\dot{\phi} \\ &+ (M_f j + M_r h + m_1 h_R)\dot{\phi}^2 + (M_f k - m_1 l_R)\dot{\phi}\dot{\psi} \\ &+ (m_1)\dot{Y}\dot{\phi}_1 + (m_1 l_R)\dot{\phi}_1^2 + (2m_1 h_R)\dot{\phi}\dot{\phi}_1 \\ &- (m_1 l_R)\dot{\phi}_1\dot{\psi} + (M_f e\sin\varepsilon)\dot{\delta}^2 - (M_f + M_r \\ &+ m_1)\dot{X}\dot{\varphi} + (M_f j + M_r h + m_1 h_R)\dot{\varphi}^2 \\ &- (M_f k - m_1 l_R)\ddot{\varphi}\end{aligned} \tag{5}$$

However, the motion in the direction z has a constraint due to the level of the ground.

While considering the rotational motion of the vehicle and the rider, the angular momenta corresponding to the front body, including the steering and front wheel, the rear body, including the rear wheel, and the rider's body are calculated. By taking the time derivatives of the angular momenta and making a summation of them, the rolling moment, pitching moment and yawing moment with respect to the x-axis, y-axis and z-axis are

$$\begin{aligned}\Sigma \boldsymbol{M}_x^i &= (M_f j + M_r h + m_1 h_R)\ddot{Y} + (M_f j^2 + M_r h^2 \\ &+ m_1 h_R^2 + I_{fs}\sin^2\varepsilon + I_{ft}\cos^2\varepsilon + I_{rx} + i_{m1x})\ddot{\phi} \\ &+ (m_1 h_R^2 + i_{m1x})\ddot{\phi}_1 + \{M_f jk + (I_{fs} - I_{ft})\sin\varepsilon\cos\varepsilon \\ &- I_{rxz} - m_1 h_R l_R\}\ddot{\psi} + \{M_f j + M_r h + m_1 h_R \\ &+ i_{fy}/R_f + (i_{ry} + i\lambda)/R_r\}\dot{X}\dot{\psi} + (M_f ej + I_{fs}\sin\varepsilon)\ddot{\delta} \\ &+ (i_{fy}/R_f\cos\varepsilon)\dot{X}\dot{\delta} + (I_{fs}\cos\varepsilon)\dot{\varphi}\dot{\delta} - (M_f j + M_r h \\ &+ m_1 h_R)\dot{Z}\dot{\phi} - (m_1 h_R)\dot{Z}\dot{\phi}_1 - (m_1 h_R l_R)\dot{\phi}_1\dot{\varphi} \\ &+ (M_f jk - m_1 h_R l_R - I_{rxz} + I_{fs}\cos\varepsilon\sin\varepsilon \\ &- I_{ft}\cos\varepsilon\sin\varepsilon)\dot{\phi}\dot{\varphi} - (M_f j^2 + M_r h^2 + m_1 h_R^2 \\ &+ I_{fy} + I_{ry} - I_{rz} + i_{m1y} - i_{m1z} - I_{fs}\cos^2\varepsilon \\ &- I_{ft}\sin^2\varepsilon)\dot{\phi}\dot{\psi}\end{aligned} \tag{6}$$

$$\begin{aligned}\Sigma \boldsymbol{M}_y^i =& -(M_f k - m_1 l_R)\ddot{Z} - (M_f k - m_1 l_R)\dot{Y}\dot{\phi} \\ &+ (m_1 l_R)\dot{Y}\dot{\phi}_1 + (m_1 h_R l_R)\dot{\phi}_1^2 + (2m_1 h_R l_R)\dot{\phi}\dot{\phi}_1 \\ &+ (M_f k - m_1 l_R)\dot{X}\phi + [M_f(j^2 - k^2) + M_r h^2 \\ &+ m_1(h_R{}^2 - l_R^2) + I_{rx} - I_{rz} + i_{m1x} - i_{m1z} \\ &+ (I_{fs} - I_{ft})(\sin^2\varepsilon - \cos^2\varepsilon)]\dot{\phi}\dot{\psi} + (m_1 h_R^2 - m_1 l_R^2 \\ &+ i_{m1x} - i_{m1z})\dot{\phi}_1\dot{\psi} + [M_f(j^2 + k^2) + M_r h^2 \\ &+ m_1(h_R^2 + l_R^2) + I_{fy} + I_{ry} + i_{m1y}]\ddot{\phi} + (M_f j \\ &+ M_r h + m_1 h_R)\dot{Y}\dot{\psi} - (M_f j + M_r h + m_1 h_R)\dot{Z}\phi \\ &+ [M_f e(j\cos\varepsilon - k\sin\varepsilon)]\dot{\delta}^2 + (I_{fs}\sin\varepsilon)\dot{\delta}\dot{\psi} \\ &- (I_{fs}\cos\varepsilon)\dot{\delta}\dot{\phi} + [M_f jk - m_1 h_R l_R - I_{rxz} \\ &+ (I_{fs} - I_{ft})\cos\varepsilon\sin\varepsilon]\dot{\psi}^2 - [M_f jk - m_1 h_R l_R \\ &- I_{rxz} + (I_{fs} - I_{ft})\cos\varepsilon\sin\varepsilon]\dot{\phi}^2 - [M_f j + M_r h \\ &+ m_1 h_R + i_{fy}/R_f + (i_{ry} + i\lambda)/R_r]\ddot{X} \end{aligned} \quad (7)$$

$$\begin{aligned}\Sigma \boldsymbol{M}_z^i =& (M_f k - m_1 l_R)\ddot{Y} + [M_f jk + (I_{fs} - I_{ft})\sin\varepsilon\cos\varepsilon \\ &- I_{rxz} - m_1 h_R l_R]\ddot{\phi} - (m_1 h_R l_R)\ddot{\phi}_1 + [M_f k^2 \\ &+ I_{fs}\cos^2\varepsilon + I_{ft}\sin^2\varepsilon + I_{rz} + m_1 l_R^2 + i_{m1z}]\ddot{\psi} \\ &+ (M_f ek + I_{fs}\cos\varepsilon)\ddot{\delta} - [i_{fy}/R_f + (i_{ry} + i\lambda)/R_r]\dot{X}\dot{\phi} \\ &+ (M_f k - m_1 l_R)\dot{X}\dot{\psi} - (i_{fy}/R_f\sin\varepsilon)\dot{X}\delta \\ &- (I_{fs}\sin\varepsilon)\dot{\delta}\phi - [M_f jk - m_1 h_R l_R + (I_{fs} \\ &- I_{ft})\sin\varepsilon\cos\varepsilon - I_{rxz}]\phi\dot{\psi} + [M_f k^2 + m_1 l_R^2 \\ &- I_{fs}\sin^2\varepsilon - I_{ft}\cos^2\varepsilon + I_{fy} + I_{ry} - I_{rx} - i_{m1x} \\ &+ i_{m1y}]\dot{\phi}\phi + (m_1 l_R^2 - i_{m1x} + i_{m1y})\dot{\phi}_1\phi \\ &- (M_f k - m_1 l_R)\dot{Z}\dot{\phi} + (m_1 l_R)\dot{Z}\dot{\phi}_1 \end{aligned} \quad (8)$$

and the steering torque with respect to the x_s-axis is

$$\begin{aligned}\Sigma \boldsymbol{M}_s^i =& (M_f e)\ddot{Y} + (M_f ej + I_{fs}\sin\varepsilon)\ddot{\phi} \\ &+ (M_f ek + I_{fs}\cos\varepsilon)\ddot{\psi} - (i_{fy}/R_f\cos\varepsilon)\dot{X}\dot{\phi} \\ &+ [M_f e(i_{fy}/R_f)\sin\varepsilon]\dot{X}\dot{\psi} - (M_f ej)\phi\dot{\psi} \\ &- (M_f e)\dot{Z}\dot{\phi} + (M_f ke)\dot{\phi}\phi + (M_f e^2 + I_{fs})\ddot{\delta} \end{aligned} \quad (9)$$

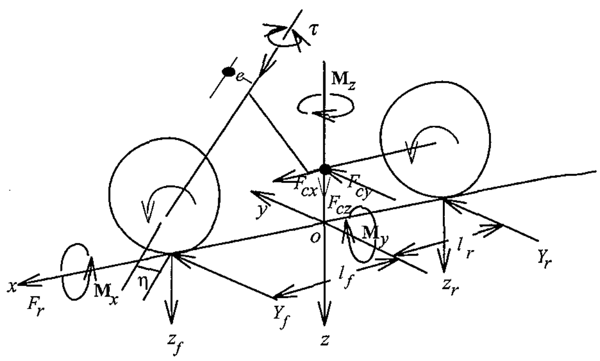

Fig. 2 The represented external forces acting on the vehicle

Rider rolling moment with respect to the x'-axis is

$$\begin{aligned}\Sigma \boldsymbol{M}_r^i =& (m_1 h_R)\ddot{Y} + (m_1 h_R^2 + i_{m1x})\ddot{\phi} + (m_1 h_R^2 \\ &+ i_{m1x})\ddot{\phi}_1 - (m_1 h_R l_R)\ddot{\psi} + m_1 h_R\dot{X}\dot{\psi} \\ &- (m_1 h_R)\dot{Z}\dot{\phi} - (m_1 h_R)\dot{Z}\dot{\phi}_1 - (m_1 h_R l_R)\dot{\phi}\phi \\ &- (m_1 h_R l_R)\dot{\phi}_1\phi - (m_1 h_R^2 + i_{m1y} - i_{m1z})\phi\dot{\psi} \\ &+ [\omega_1^2(m_1 h_R^2 + i_{m1x})]\sin\phi_1 + [2\zeta_1\omega_1(m_1 h_R^2 \\ &+ i_{m1x})]\sin\dot{\phi}_1 \end{aligned} \quad (10)$$

According to Eq. (10), the last two terms are generated with the stiffness of rider action which is referred to in Katayama's model (1988). The tire forces are

$$\begin{aligned} Y_f =& -C_{ys1}(\dot{Y}/\dot{X}) - C_{ys1}l_f(\dot{\psi}/\dot{X}) + C_{ys1}\eta(\dot{\delta}/\dot{X}) \\ &+ C_{yc1}\phi + (C_{ys1}\cos\varepsilon + C_{yc1}\sin\varepsilon)\delta \end{aligned} \quad (11)$$

$$Y_r = -C_{ys2}(\dot{Y}/\dot{X}) + C_{ys2}l_r(\dot{\psi}/\dot{X}) + C_{yc2}\phi \quad (12)$$

which are referred to in Weir and Zellner (1978) and Chang (1992). However, Eqs. (11) and (12) are, in the case of Katayama's model (1988), neglecting $\dot{Y}_f$, $\dot{Y}_r$ due to their small influence.

Assume that a force F_c, at an angle (θ_x, θ_y, θ_z) merely hits the motorcycle at (r_{cx}, r_{cy}, r_{cz}) of the x-y-z coordinate system. In addition, F_c has components F_{cx}, F_{cy} and F_{cz} where, $F_{cx}=F_c\sin\theta_x$, $F_{cy}=F_c\cos\theta_y$ and $F_{cz}=F_c\cos\theta_z$. If acting on the rear body, the force produces moments, $F_{cz}r_{cz}-F_{cy}r_{cz}$ for rolling motion, $F_{cx}r_{cz}-F_{cz}r_c$ for pitching motion and $F_{cy}r_{cx}-F_{cx}r_{cy}$ for yawing motion. If the force is acting upon the front body, aside from the effects for rolling, pitching and yawing motion described above, there is a moment eF_{cy} produced for the steering motion. Fig. 2 illustrates the represented external forces that are a longitudinal force, lateral force, rolling moment, yawing moment, steering moment, and the rolling moment with respect to the rider.

Based on the gravity, collision force, traction force, and steering torque applied by the rider, we have the longitudinal force:

$$\Sigma \boldsymbol{F}_x^e = -F_r + F_{cx} + F_d \tag{13}$$

lateral force,

$$\Sigma \boldsymbol{F}_y^e = Y_f + Y_r + F_{cy} \tag{14}$$

vertical force,

$$\Sigma \boldsymbol{F}_z^e = (M_f + M_r + m_1)g + F_{cz} + Z_f + Z_r \tag{15}$$

rolling moment,

$$\Sigma \boldsymbol{M}_x^e = (M_f j + M_r h + m_1 h_R) g \sin\phi + m_1 h_R g \sin\phi_1 - (\eta Z_f - M_f e g)\sin\delta + F_{cz} r_{cy} - F_{cy} r_{cz} \tag{16}$$

pitching moment,

$$\Sigma \boldsymbol{M}_y^e = F_{cx} r_{cz} - F_{cz} r_{cx} - l_f Z_f + l_r Z_r - M_f g k + m_1 g l_R \tag{17}$$

yawing moment,

$$\Sigma \boldsymbol{M}_z^e = F_{cy} r_{cx} - F_{cx} r_{cy} - \tau\cos\varepsilon + l_f Y_f - l_r Y_r \tag{18}$$

steering moment,

$$\boldsymbol{M}_s^e = -(\eta Z_f - M_f e g)\sin\phi - (\eta Z_f - M_f e g)\sin\varepsilon \sin\delta + \tau - \eta Y_f + e F_{cy} \tag{19}$$

However, if the collision is on the rear body, the remaining term in the above equation vanishes. In addition, the rolling moment with respect to the rider is

$$\Sigma \boldsymbol{M}_r^e = m_1 h_R \sin\phi + m_1 h_R g \sin\phi_1 - \tau\sin\varepsilon \tag{20}$$

4. System Dynamic Equation

By applying Eqs. (1)~(20), the equilibrium between the internal inertia and external forces is satisfied as follows:

(i) Longitudinal equilibrium: $\Sigma \boldsymbol{F}_x^i = \Sigma \boldsymbol{F}_x^e$

$$\begin{aligned}
&(M_f + M_r + m_1)\ddot{X} - (M_f + M_r + m_1)\dot{Y}\dot{\psi} - (M_f j \\
&+ M_r h + m_1 h_R)\dot{\phi}\dot{\psi} - (m_1 h_R)\dot{\phi}_1\dot{\psi} - (M_f k - m_1 l_R)\dot{\psi}^2 \\
&- (M_f e \cos\varepsilon)\dot{\delta}^2 - (M_f j + M_r h + m_1 h_R)\ddot{\varphi} \\
&+ (M_f + M_r + m_1)\dot{Z}\dot{\varphi} - (M_f k - m_1 l_R)\dot{\varphi}^2 \\
&= -F_r + F_{cx} + F_d
\end{aligned} \tag{21}$$

(ii) Lateral equilibrium: $\Sigma \boldsymbol{F}_y^i = \Sigma \boldsymbol{F}_y^e$

$$\begin{aligned}
&(M_f + M_r + m_1)\ddot{Y} + (M_f j + M_r h + m_1 h_R)\ddot{\phi} + (m_1 h_R)\ddot{\phi}_1 \\
&+ (M_f k - m_1 l_R)\ddot{\psi} + (M_f e)\ddot{\delta} + (M_f + M_r + m_1)\dot{X}\dot{\psi} \\
&- (M_f j + M_r h + m_1 h_R)\dot{\varphi}\dot{\psi} - (M_f + M_r + m_1)\dot{Z}\dot{\phi} \\
&- (m_1)\dot{Z}\dot{\phi}_1 + (M_f k - m_1 l_R)\dot{\phi}\dot{\varphi} - (m_1 l_R)\dot{\phi}_1\dot{\varphi} \\
&+ (C_{ys1} + C_{ys2})\dot{Y}/\dot{X} + (C_{ys1} l_f - C_{ys2} l_r)\dot{\psi}/\dot{X} \\
&- (C_{ys1}\eta)\dot{\delta}/\dot{X} - (C_{ys1}\cos\varepsilon + C_{yc1}\sin\varepsilon)\delta - (C_{yc1} + C_{yc2})\phi \\
&= F_{cy}
\end{aligned} \tag{22}$$

(iii) Vertical equilibrium: $\Sigma \boldsymbol{F}_z^i = \Sigma \boldsymbol{F}_z^e$

$$\begin{aligned}
&(M_f + M_r + m_1)\ddot{Z} - (M_f k - m_1 l_R)\ddot{\varphi} + (M_f + M_r + m_1)\dot{Y}\dot{\phi} \\
&(M_f j + M_r h + m_1 h_R)\dot{\phi}^2 + (M_f k - m_1 l_R)\dot{\phi}\dot{\psi} + (m_1)\dot{Y}\dot{\phi}_1 \\
&+ (m_1 h_R)\dot{\phi}_1^2 + (2 m_1 h_R)\dot{\phi}\dot{\phi}_1 - (m_1 l_R)\dot{\phi}_1\dot{\psi} + (M_f e \sin\varepsilon)\dot{\delta}^2 \\
&- (M_f + M_r + m_1)\dot{X}\dot{\varphi} + (M_f j + M_r h + m_1 h_R)\dot{\varphi}^2 \\
&= (M_f + M_r + m_1)g + F_{cz} + Z_f + Z_r
\end{aligned} \tag{23}$$

(iv) Rolling equilibrium: $\Sigma \boldsymbol{M}_x^i = \Sigma \boldsymbol{M}_x^e$

$$\begin{aligned}
&(M_f j + M_r h + m_1 h_R)\ddot{Y} + (M_f j^2 + M_r h^2 + m_1 h_R^2 \\
&+ I_{fs}\sin^2\varepsilon + I_{ft}\cos^2\varepsilon + I_{rx} + i_{m1x})\ddot{\phi} + (m_1 h_R^2 + i_{m1x})\ddot{\phi}_1 \\
&+ \{M_f jk + (I_{fs} - I_{ft})\sin\varepsilon\cos\varepsilon - I_{rxz} - m_1 h_R l_R\}\ddot{\psi} \\
&+ \{M_f j + M_r h + m_1 h_R + i_{fy}/R_f + (i_{ry} + i\lambda)/R_r\}\dot{X}\dot{\psi} \\
&+ (M_f e j + I_{fs}\sin\varepsilon)\ddot{\delta} + (i_{fy}/R_y\cos\varepsilon)\dot{X}\dot{\delta} + (I_{fs}\cos\varepsilon)\dot{\varphi}\dot{\delta} \\
&- (M_f j + M_r h + m_1 h_R)\dot{Z}\dot{\phi} - (m_1 h_R)\dot{Z}\dot{\phi}_1 - (m_1 h_R l_R)\dot{\phi}_1\dot{\varphi} \\
&+ (M_f jk - m_1 h_R l_R - I_{rxz} + I_{fs}\cos\varepsilon\sin\varepsilon - I_{ft}\cos\varepsilon\sin\varepsilon)\dot{\phi}\dot{\varphi} \\
&- (M_f j^2 + M_r h^2 + m_1 h_R^2 + I_{fy} + I_{ry} - I_{rz} + i_{m1y} - i_{m1z} \\
&- I_{fs}\cos^2\varepsilon - I_{ft}\sin^2\varepsilon)\dot{\varphi}\dot{\psi} - \{(M_f j + M_r h + m_1 h_R)g\}\phi \\
&- (m_1 h_R g)\phi_1 + (\eta Z_f - M_f e g)\delta \\
&= F_{cz} r_{cy} - F_{cy} r_{cz}
\end{aligned} \tag{24}$$

(v) Pitching equilibrium: $\Sigma \boldsymbol{M}_y^i = \Sigma \boldsymbol{M}_y^e$

$$-(M_fk-m_1l_R)\ddot{Z}-(M_fk-m_1l_R)\dot{Y}\dot{\phi}+(m_1l_R)\dot{Y}\dot{\phi}_1$$

$$+(m_1h_Rl_R)\dot{\phi}_1^2+(2m_1h_Rl_R)\dot{\phi}\dot{\phi}_1+(M_fk-m_1l_R)\dot{X}\dot{\varphi}$$

$$+[M_f(j^2-k^2)+M_rh^2+m_1(h_R^2-l_R^2)+I_{rx}-I_{rz}$$

$$+i_{m1x}-i_{m1z}+(I_{fs}-I_{ft})(\sin^2\varepsilon-\cos^2\varepsilon)]\dot{\phi}\dot{\psi}$$

$$+(m_1h_R^2-m_1l_R^2+i_{m1x}-i_{m1z})\dot{\phi}_1\dot{\psi}+[M_f(j^2+k^2)$$

$$+M_rh^2+m_1(h_R^2+l_R^2)+I_{fy}+I_{ry}+i_{m1y}]\ddot{\varphi}$$

$$+(M_fj+M_rh+m_1h_R)\dot{Y}\dot{\psi}-(M_fj+M_rh+m_1h_R)\dot{Z}\dot{\varphi}$$

$$+[M_fe(j\cos\varepsilon-k\sin\varepsilon)]\dot{\delta}^2+(I_{fs}\sin\varepsilon)\dot{\delta}\dot{\psi}-(I_{fs}\cos\varepsilon)\dot{\delta}\dot{\phi}$$

$$+[M_fjk-m_1h_Rl_R-I_{rxz}+(I_{fs}-I_{ft})\cos\varepsilon\sin\varepsilon]\dot{\psi}^2$$

$$-[M_fjk-m_1h_Rl_R-I_{rxz}+(I_{fs}-I_{ft})\cos\varepsilon\sin\varepsilon]\dot{\phi}^2$$

$$-[M_fj+M_rh+m_1h_R+i_{fy}/R_y+(i_{ry}+i\lambda)/R_r]\ddot{X}$$

$$=F_{cx}r_{cz}-F_{cz}r_{cx}-l_fZ_f+l_rZ_r-M_fgk+m_1gl_R \tag{25}$$

(vi) Yawing equilibrium: $\sum M_z^i=\sum M_z^e$

$$(M_fk-m_1l_R)\ddot{Y}+[M_fjk+(I_{fs}-I_{ft})\sin\varepsilon\cos\varepsilon-I_{rxz}$$

$$-m_1h_Rl_R]\ddot{\phi}-(m_1h_Rl_R)\ddot{\phi}_1+[M_fk^2+I_{fs}\cos^2\varepsilon$$

$$+I_{ft}\sin^2\varepsilon+I_{rz}+m_1l_R^2+i_{m1z}]\ddot{\psi}+(M_fek+I_{fs}\cos\varepsilon)\ddot{\delta}$$

$$-[i_{fy}/R_f+(i_{ry}+i\lambda)/R_r]\dot{X}\dot{\phi}+(M_fk-m_1l_R)\dot{X}\dot{\psi}$$

$$-(i_{fy}/R_f\sin\varepsilon)\dot{X}\dot{\delta}-(I_{fs}\sin\varepsilon)\dot{\delta}\dot{\varphi}-[M_fjk-m_1h_Rl_R$$

$$+(I_{fs}-I_{ft})\sin\varepsilon\cos\varepsilon-I_{rxz}]\dot{\varphi}\dot{\psi}+[M_fk^2+m_1l_R^2$$

$$-I_{fs}\sin^2\varepsilon-I_{ft}\cos^2\varepsilon+I_{fy}+I_{ry}-I_{rx}-i_{m1x}+i_{m1y}]\dot{\phi}\dot{\varphi}$$

$$+(m_1l_R^2-i_{m1x}+i_{m1y})\dot{\phi}_1\dot{\varphi}-(M_fk-m_1l_R)\dot{Z}\dot{\phi}$$

$$+(m_1l_R)\dot{Z}\dot{\phi}_1+(l_fC_{ys1}-l_yC_{ys2})\dot{Y}/\dot{X}+(l_f^2C_{ys1}$$

$$+l_r^2C_{ys2})\dot{\psi}/\dot{X}-(l_f\eta C_{ys1})\dot{\delta}/\dot{X}-\{l_f(C_{ys1}\cos\varepsilon$$

$$+C_{yc1}\sin\varepsilon)\}\delta-(l_fC_{yc1}-l_rC_{yc2}+a\cos\varepsilon)\phi-(b\cos\varepsilon)\dot{\phi}$$

$$=F_{cy}r_{cx}-F_{cx}r_{cy} \tag{26}$$

(vii) Steering equilibrium: $\sum M_s^i=\sum M_s^e$

$$(M_fe)\ddot{Y}+(M_fej+I_{fs}\sin\varepsilon)\ddot{\phi}+(M_fek+I_{fs}\cos\varepsilon)\ddot{\psi}$$

$$-(i_{fy}/R_f\cos\varepsilon)\dot{X}\dot{\phi}+[M_fe+(i_{fy}/R_f)\sin\varepsilon]\dot{X}\dot{\psi}$$

$$-(M_fej)\dot{\varphi}\dot{\psi}-(M_fe)\dot{Z}\dot{\phi}+(M_fke)\dot{\phi}\dot{\varphi}+(M_fe^2+I_{fs})\ddot{\delta}$$

$$+(\eta Z_f-M_feg+\eta C_{yc1}+a)\phi+b\dot{\phi}-(\eta C_{ys1})\dot{Y}/\dot{X}$$

$$-(\eta C_{ys1}l_f)\dot{\psi}/\dot{X}+(\eta^2C_{ys1})\dot{\delta}/\dot{X}+\{\eta(C_{ys1}\cos\varepsilon$$

$$+C_{yc1}\sin\varepsilon)+(\eta Z_f-M_feg)\sin\varepsilon\}\delta$$

$$=eF_{cy} \tag{27}$$

The right-hand term vanishes if the collision acts upon the rear body.

(viii) Rider rolling equilibrium: $\sum M_r^i=\sum M_r^e$

$$(m_1h_R)\ddot{Y}+(m_1h_R^2+i_{m1x})\ddot{\phi}+(m_1h_R^2+i_{m1x})\ddot{\phi}_1$$

$$-(m_1h_Rl_R)\ddot{\psi}+m_1h_R\dot{X}\dot{\psi}-(m_1h_R)\dot{Z}\dot{\phi}_1-(m_1h_Rl_R)\dot{\phi}\dot{\varphi}$$

$$-(m_1h_Rl_R)\dot{\phi}_1\dot{\varphi}-(m_1h_R^2+i_{m1y}-i_{m1z})\dot{\varphi}\dot{\psi}$$

$$+[(\omega_1^2(m_1h_R^2+i_{m1x})-m_1h_Rg]\phi_1+[2\zeta_1\omega_1(m_1h_R^2$$

$$+i_{m1x})]\dot{\phi}_1-(m_1h_Rg+a\sin\varepsilon)\phi-(b\sin\varepsilon)\dot{\phi}$$

$$=0 \tag{28}$$

III. SOLVING ALGORITHM

In the previous section, eight equations, Eqs. (21)-(28), represent the system dynamic equation of an impacted motorcycle. The system is obviously nonlinear and quite elaborate. A time-scanning simulation is used to investigate such an elaborate system's trajectory for measurement or assessment. Without a loss of generality, in a tiny time interval, this study linearizes the equation and uses a discrete form to simulate the system.

By incorporating Eqs. (21)-(28), briefly in symbols the system equation can be expressed in the following matrix form:

$$\boldsymbol{A}\ddot{\boldsymbol{X}}(t)=f(\dot{\boldsymbol{X}}(t),\boldsymbol{X}(t),t) \tag{29}$$

where

$\boldsymbol{X}(t)=[Y\ \phi\ \psi\ \delta\ \phi_1\ X\ Z\ \varphi]^T$, the vector of system variables;

$\boldsymbol{A}=[a_{ij}]$, i=1, 2, ..., 8; j=1, 2, ..., 8, the coefficient matrix of vector $\ddot{\boldsymbol{X}}(t)$.

where t denotes the time coordinate. In a tiny time interval T, the linearity of Eq. (29) is taken, thereby implying

$$\boldsymbol{A}\ddot{\boldsymbol{X}} = \boldsymbol{B}\dot{\boldsymbol{X}} + \boldsymbol{C}\boldsymbol{X} + \boldsymbol{D} \tag{30}$$

where $\boldsymbol{A}$, $\boldsymbol{B}$, $\boldsymbol{C}$ and $\boldsymbol{D}$ are coefficient matrices in terms of state original $\boldsymbol{X}$ and $\dot{\boldsymbol{X}}$ (denoted as $\boldsymbol{X}_0$ and $\dot{\boldsymbol{X}}_o$) in an interval. Within an interval T, these coefficients are obviously assumed to be constants; however, they vary when the state changes. However, Eq. (30) can not be solved directly because the coefficient matrices may be singular under certain given conditions of Eqs. (21)-(28). A partitioning method is involved in the solution process. In such a case, let's partition $\boldsymbol{X}$ into two sub-vectors:

$$\boldsymbol{x}_1=[Y\ \phi\ \psi\ \delta\ \phi_1]^T$$

$$\boldsymbol{x}_2=[X\ Z\ \varphi]^T$$

Putting Eqs. (22), (24), (26)-(28) in a group yields

$$\boldsymbol{A}_1\ddot{\boldsymbol{X}}_1 = \boldsymbol{B}_1\dot{\boldsymbol{x}}_1 + \boldsymbol{C}_1\boldsymbol{x}_1 + f_1(\dot{\boldsymbol{x}}_2; \boldsymbol{d}_1) \tag{31}$$

$\boldsymbol{A}_1$, $\boldsymbol{B}_1$, $\boldsymbol{C}_1$ are coefficient matrices in terms of state initial $\boldsymbol{X}_o$ and $\dot{\boldsymbol{X}}_o$. $f_1(\dot{\boldsymbol{x}}_2; \boldsymbol{d}_1)$ is a function of $\dot{\boldsymbol{x}}_2$ with a constant term $\boldsymbol{d}_1$ in a state. The other group formed with Eqs. (21), (23) and (25) yields

$$\boldsymbol{A}_2\ddot{\boldsymbol{X}}_2 = \boldsymbol{B}_2\dot{\boldsymbol{x}}_2 + f_2(\dot{\boldsymbol{x}}_1; \boldsymbol{d}_2) \tag{32}$$

In addition, $\boldsymbol{A}_2$, $\boldsymbol{B}_2$ are also coefficient matrices in terms of state initial $\boldsymbol{X}_o$ and $\dot{\boldsymbol{X}}_o$. $f_2(\dot{\boldsymbol{x}}_1; \boldsymbol{d}_2)$ is a function of $\dot{\boldsymbol{x}}_1$ with a constant term $\boldsymbol{d}_2$ in a state.

The solution process initially involves solving Eq. (31) in an interval given $f_1(\dot{\boldsymbol{x}}_2; \boldsymbol{d}_1)$ at an initial condition $\dot{\boldsymbol{x}}_2 = \dot{\boldsymbol{x}}_{2o}$. Let

$$\boldsymbol{y}_1 = \boldsymbol{x}_1$$

$$\boldsymbol{y}_2 = \dot{\boldsymbol{y}}_1 = \dot{\boldsymbol{x}}_1 \tag{33}$$

which implies

$$\dot{\boldsymbol{y}}_1 = \boldsymbol{y}_2$$

$$\dot{\boldsymbol{y}}_2 = \ddot{\boldsymbol{y}}_1 = \ddot{\boldsymbol{x}}_1 = \boldsymbol{A}_1^{-1}\boldsymbol{B}_1\boldsymbol{y}_2 + \boldsymbol{A}_1^{-1}\boldsymbol{C}_1\boldsymbol{y}_1 + \boldsymbol{A}_1^{-1}f_1(\dot{\boldsymbol{x}}_{2o}; \boldsymbol{d}_1) \tag{34}$$

The state space expression of Eq. (31) is expressed as

$$\begin{bmatrix}\dot{\boldsymbol{y}}_1\\ \dot{\boldsymbol{y}}_2\end{bmatrix} = \begin{bmatrix}\boldsymbol{0} & \boldsymbol{1}\\ \boldsymbol{A}_1^{-1}\boldsymbol{C}_1 & \boldsymbol{A}_1^{-1}\boldsymbol{B}_1\end{bmatrix}\begin{bmatrix}\boldsymbol{y}_1\\ \boldsymbol{y}_2\end{bmatrix} + \begin{bmatrix}\boldsymbol{0}'\\ \boldsymbol{A}_1^{-1}f_1(\dot{\boldsymbol{x}}_{2o}; d_1)\end{bmatrix} \tag{35}$$

where $\boldsymbol{0}$ and $\boldsymbol{1}$ denote a zero matrix and identity matrix, respectively. $\boldsymbol{0}'$ denotes a zero column vector with five elements. Referring back to the symbols in Eq. (33), the solution of Eq. (35) is

$$\begin{bmatrix}\boldsymbol{x}_1\\ \dot{\boldsymbol{x}}_1\end{bmatrix} = \exp(\begin{bmatrix}\boldsymbol{0} & \boldsymbol{1}\\ \boldsymbol{A}_1^{-1}\boldsymbol{C}_1 & \boldsymbol{A}_1^{-1}\boldsymbol{B}_1\end{bmatrix}t)\cdot\begin{bmatrix}\boldsymbol{x}_{1o}\\ \dot{\boldsymbol{x}}_{1o}\end{bmatrix} - \begin{bmatrix}\boldsymbol{0} & \boldsymbol{1}\\ \boldsymbol{A}_1^{-1}\boldsymbol{C}_1 & \boldsymbol{A}_1^{-1}\boldsymbol{B}_1\end{bmatrix}^{-1}\begin{bmatrix}\boldsymbol{0}'\\ \boldsymbol{A}_1^{-1}f_1(\dot{\boldsymbol{x}}_{2o}; \boldsymbol{d}_1)\end{bmatrix} \tag{36}$$

where t is in the interval T. In the same manner, the solution of Eq. (32) is

$$\dot{\boldsymbol{x}}_2 = \exp(\boldsymbol{A}_1^{-1}\boldsymbol{B}_2 t)\cdot\dot{\boldsymbol{x}}_{2o} - (\boldsymbol{A}_1^{-1}\boldsymbol{B}_2)^{-1}\boldsymbol{A}_2^{-1}f_2(\dot{\boldsymbol{x}}_{1o}; \boldsymbol{d}_2) \tag{37}$$

By taking a tiny T, the state transfer functions with step expression for Eqs. (36) and (37) are, respectively, approximate to:

$$\begin{bmatrix}\boldsymbol{x}_1(n+1)\\ \dot{\boldsymbol{x}}_1(n+1)\end{bmatrix} = (\boldsymbol{I}_1 + \begin{bmatrix}\boldsymbol{0} & \boldsymbol{1}\\ \boldsymbol{A}_1^{-1}\boldsymbol{C}_1 & \boldsymbol{A}_1^{-1}\boldsymbol{B}_1\end{bmatrix}T)\cdot\begin{bmatrix}\boldsymbol{x}_1(n)\\ \dot{\boldsymbol{x}}_1(n)\end{bmatrix} - \begin{bmatrix}\boldsymbol{0} & \boldsymbol{1}\\ \boldsymbol{A}_1^{-1}\boldsymbol{C}_1 & \boldsymbol{A}_1^{-1}\boldsymbol{B}_1\end{bmatrix}^{-1}\begin{bmatrix}\boldsymbol{0}'\\ \boldsymbol{A}_1^{-1}f_1(\dot{\boldsymbol{x}}_2(n); \boldsymbol{d}_1)\end{bmatrix} \tag{38}$$

$$\dot{\boldsymbol{x}}_2(n+1) = [\boldsymbol{I}_2 + (\boldsymbol{A}_2^{-1}\boldsymbol{B}_2)T]\cdot\dot{\boldsymbol{x}}_2(n) - \boldsymbol{B}_2^{-1}f_2(\dot{\boldsymbol{x}}_1(n); \boldsymbol{d}_2) \tag{39}$$

where $\boldsymbol{I}_1$ and $\boldsymbol{I}_2$ denote the identity matrix with ten square elements and three square elements, respectively. According to Eqs. (31) and (32), the acceleration can be calculated and, also, the new position at state (n+1) found if the original position (X,Y, Z) at state n is known. Eqs. (38) and (39) reveal the transfer from the beginning of a state to the end of the state. Because all coefficients vary when the state changes, new $\boldsymbol{A}_1$, $\boldsymbol{B}_1$, $\boldsymbol{C}_1$, and $\boldsymbol{A}_2$, $\boldsymbol{B}_2$ as well as $\boldsymbol{d}_1$, $\boldsymbol{d}_2$ at state (n+1) are determined by the state-ended results of Eqs. (38) and (39) at state n. Thus, given initial values at state 0, each variation of the system can then be simulated by Eqs. (38) and (39) iteratively from time to time.

The partitioning method does not ensure the result in an initiated condition with all zeros. The Runge-Kutta method can be an option to resolve this situation (Forsythe *et al.*, 1997).

However, in the iteration of simulation, steering angle δ, steering torque τ and roll angle ϕ have their limits due to the vehicle's structural frame. In this study, we make the following defaults:

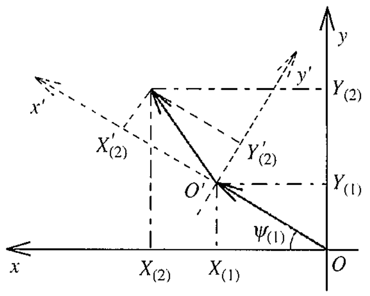

Fig. 3 Moving vector returning to the original coordinate system

(i) Steering angle has an upper limit absolute value of 45°. When the steering reaches the limit, the steering rate is set to zero. Simultaneously, the steering torque is also at zero level;

(ii) Steering torque τ is a function of rolling angle ϕ and rolling velocity $\dot{\phi}$. When the rolling angle reaches 30°, the driver loses his/her handling capability for the vehicle, i.e. the steering torque is at zero state; and

(iii) When the roll angle reaches 90°, the vehicle is defined as in an overturned state. At this moment, the iterative program is terminated. This expresses that the sliding situation is outside our simulation.

According to the simulation mentioned earlier, twenty-four time-response illustrations are depicted for demonstrating the dynamic behaviors of the proposed model, which include motion, velocity and acceleration with respect to longitudinal, lateral, vertical, pitching, yawing, vehicle rolling, rider rolling, and steering variations. In addition, a surface diagram xy is revealed for investigating vehicle tracking. However, the vehicle track output, after an impact, in each mimic interval described above, should be clarified and returned to the original continuous status. By assuming that the slipping effect at the original point 'O' is neglected, the coordinate transformation justifies the illustration of Fig. 3. According to this figure, we have

$$X_{(2)} = X_{(1)} + X'_{(2)}\cos\psi_{(1)} - Y'_{(2)}\sin\psi_{(1)} \quad (40)$$

At any state,

$$X_{(n+1)}\ X_{(n)} + X'_{(n+1)}\cos\psi_{(n)} - Y'_{(n+1)}\sin\psi_{(n)} \quad (41)$$

Similarly,

$$Y_{(n+1)} = Y_{(n)} + X'_{(n+1)}\sin\psi_{(n)} + Y'_{(n+1)}\cos\psi_{(n)} \quad (42)$$

IV. AN ILLUSTRATIVE EXAMPLE

As is generally known, if the influence from an external impact force is within the driver's control range, the driver can use steering torque to maneuver his/her vehicle to avert overturning. If the impact is out of that range, the vehicle finally overturns. A different driver with a certain motorcycle yields a different critical impact force. The above dynamic model is more clearly examined by selecting a popular motorcycle brand in Taiwan for evaluation. Table 1 lists such a motorcycle's parameters and the values, which are applied in the following simulation and analysis. In addition, according to the calibration by Wang (1997), the steering torque function of

$$\tau_{one} = -75\phi - 60\dot{\phi} \quad (43)$$

is accepted as representing the median driver's capability in Taiwan.

A demonstrative case is presented as follows. Assume that a motorcycle with the characteristics in Table 1 is driven by a rider with the capability of Eq. (43). When the speed is around 30 kph, a force of 1,500 N (Newtons, approximate 150 kg) with a level angle -30° hits the motorcycle at the position $(0\hat{\imath} - 0.05\hat{\jmath} - 0.536\hat{k})$ and lasts for only 0.2 seconds (200 ms). In this case, by applying Eq. (29) with the solving algorithm described in the previous section, twenty-four time-response trajectory plots, (including longitudinal, lateral, vertical, pitching, yawing, vehicle rolling, rider rolling, steering motion, each with respect to displacement, velocity and acceleration,) and a surface diagram of vehicle tracking are simulated. Figs. 4~12 depict portions of the simulated illustrations.

Table 1 A motorcycle model and rider's parameter values

Symbols	Values	Symbols	Values
C_{ys1}	3,481 N/rad	I_{fy}	3.9 kgm^2
C_{ys2}	4,436 N/rad	I_{fs}	0.84 kgm^2
C_{yc1}	275 N/rad	I_{ft}	3.70 kgm^2
C_{yc2}	73 N/rad	I_{rx}	11.86 kgm^2
e	0.048 m	I_{ry}	30.0 kgm^2
h	0.536 m	I_{rz}	25.77 kgm^2
h_R	1.05 m	i_{m1x}	4.5 kgm^2
j	0.562 m	i_{m1y}	4.2 kgm^2
k	0.668 m	i_{m1z}	2.62 kgm^2
l_f	0.803 m	i_{fy}	0.44 kgm^2
l_r	0.550 m	i_{ry}	0.6 kgm^2
l_R	0.111 m	m_1	65 kg
R_f	0.299 m	M_f	30.87 kg
R_r	0.312 m	M_r	166.6 kg
η	0.086 m	ε	0.4712 rad
I_{rxz}	0.0 kgm^2	λ	0.0
g	9.81 m/sec^2	ω_1	3.0 Hz
---	---	ζ_1	0.3

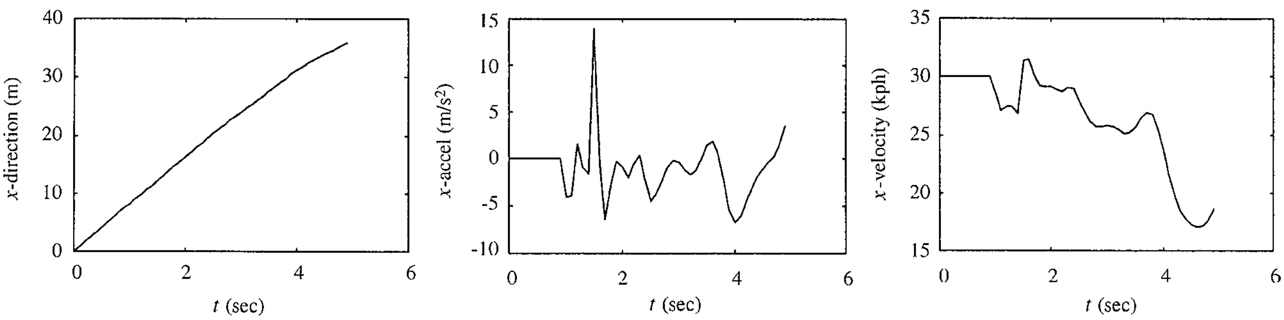

Fig. 4 Time response plots of the presented case: Longitudinal Moving

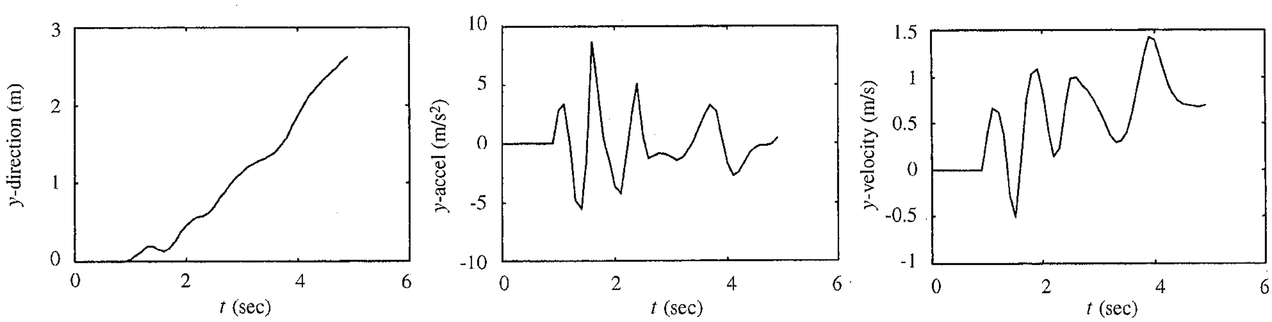

Fig. 5 Time response plots of the presented case: Lateral Displacement

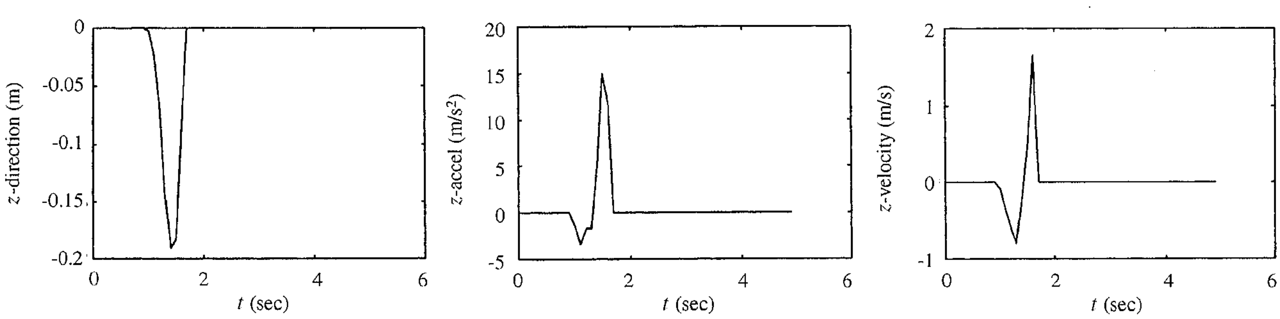

Fig. 6 Time response plots of the presented case: Vertical Moving

According to these figures, the collision occurs at 1.0 second after the beginning of our simulation. At the moment of impact, the vehicle suddenly decelerates (Fig. 4) and produces an enormous lateral acceleration (Fig. 5); however, it still moves forward but slightly turns to the right (Fig. 5, y-value is positive) and (Fig. 12). Thereafter, the vehicle's velocity becomes unstable due to the evoking and releasing of energy from an external impact. The vehicle then falls down at 5.0 sec. When falling, its approaching speed is about 19 *kph* (Fig. 4) and lateral velocity is approximate 0.65 m/s to the right (Fig. 5). This finding suggests that the vehicle slides after falling. According to Fig. 6, the vehicle obviously heaves and sinks. Fig. 7 reveals that, at first, the vehicle slightly rolls to the right but due to steering right; the vehicle finally falls to the left. Fig. 11 indicates that the rider leans to the same side. Fortunately, the leaning is only approximate 10 degrees when the vehicle falls down. This finding suggests that the rider's head does not directly hit the ground. From the cluttered steering phenomena in acceleration in Fig. 10, the rider is unable to handle the steering after impact. As for yawing behavior (Fig. 9), the vehicle first turns right for a little while, but then turns toward the left. The vehicle wobbles and weaves severely. In the final second, the yaw angle reaches approximately -200 degrees, a reverse turn (Figs. 9 and 12). Closely examining Fig. 8 reveals that the vehicle turns upside down. This coincides with the phenomenon in Fig. 9. According to Fig. 12, the vehicle finally falls 23.5 meters ahead of the impact point and 9 meters away from original centerline.

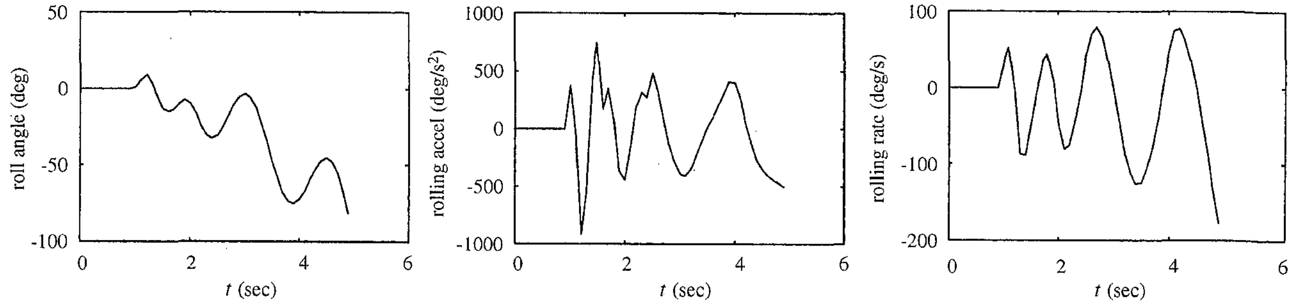

Fig. 7 Time response plots of the presented case: Rolling Variation

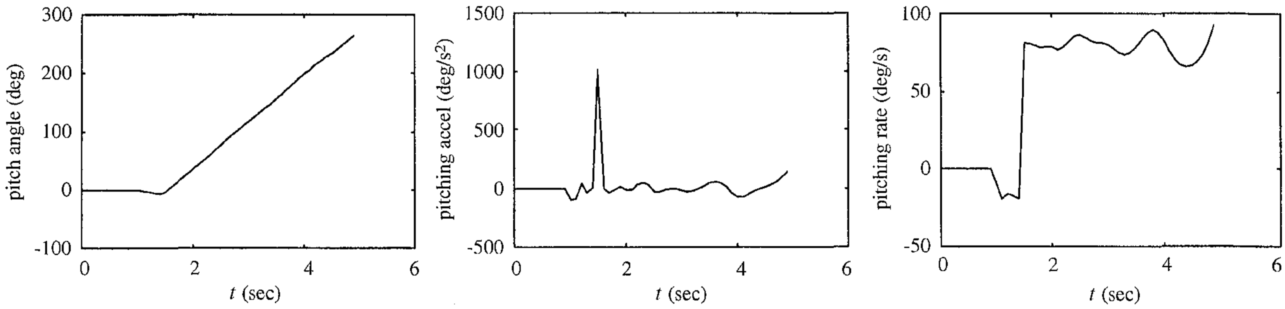

Fig. 8 Time response plots of the presented case: Pitching Variation

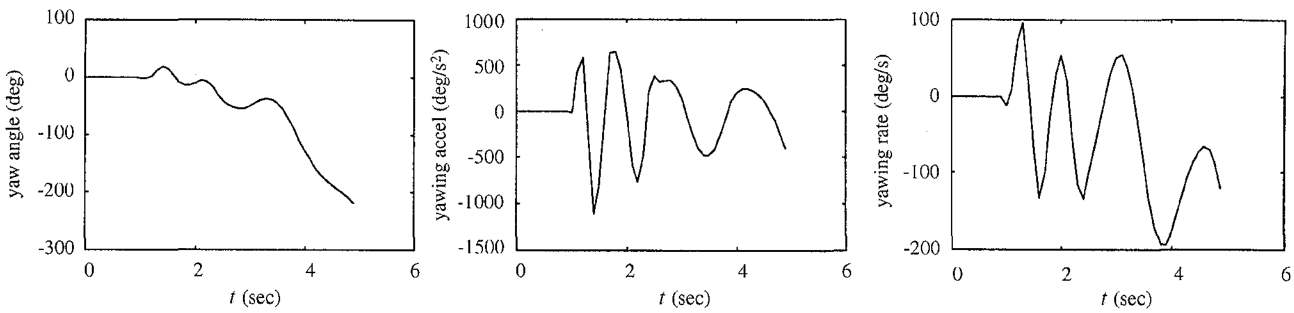

Fig. 9 Time response plots of the presented case: Yawing Variation

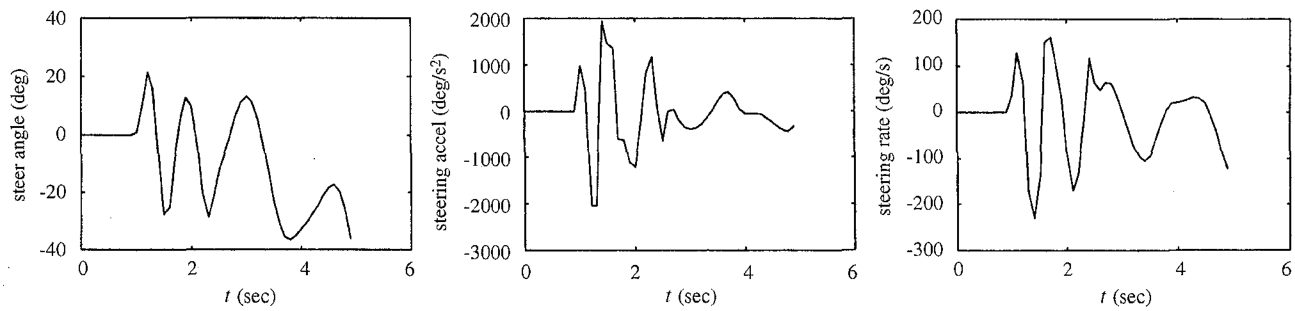

Fig. 10 Time response plots of the presented case: Steering Variation

V. CONCLUSION

Investigating a motorcycle accident is extremely difficult due to high degrees of freedom of motion in motorcycles. A reasonably accurate analytical tool for motorcycle collisions is lacking. However, developing such a tool is particularly relevant for many developing countries, particularly, in the Asia-Pacific areas. In such a tool, accurately modeling a mathematical description is of primary concern. This study

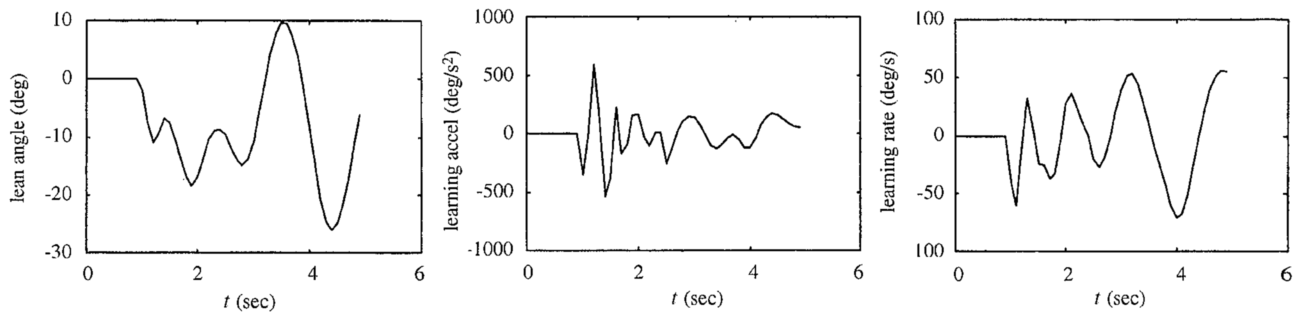

Fig. 11 Time response plots of the presented case: Rider Leaning Variation

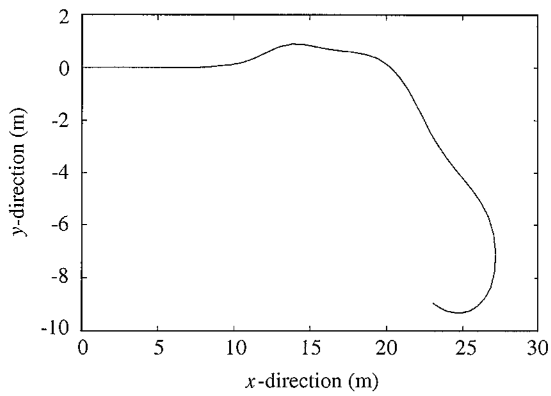

Fig.12 Surface moving of the after-impact vehicle

successfully devises an eight-degrees-of-freedom motorcycle-rider and two-wheeled vehicle dynamic model for after-impact studies. Twenty-four time-response illustrations are presented for the motion behaviors, including longitudinal, lateral, vertical, pitching, yawing, vehicle rolling, rider rolling, steering motion and their velocities, as well as a surface diagram of vehicle tracking. Simulation results indicate that the motion of an impacted motorcycle can be easily traced to obtain an explanation for the collision. Referring to the presented example, the model proposed herein can be well utilized to preliminarily analyze the behavioral tendency of a motorcycle after a collision.

Vehicle collision analysis can obviously be divided into three phases: pre-collision, colliding and after collision. The proposed model is only useful for a collision incident, and no secondary impact is involved. Therefore, the model proposed herein is insufficient for the complete investigation of motorcycle accidents. Further study should extend the model to describe a complete event and, then be widely applied towards investigating and analyzing accidents.

NOMENCLATURE

C_{yc1}, C_{yc2}	Camber stiffness of the front wheels and rear wheels
C_{ys1}, C_{ys2}	Cornering stiffness of the front wheels and rear wheels
e	Distance between the front body center of mass and steering axis (x_s-axis)
F_d	Driving force
F_r	Resistance force
g	Gravity acceleration
H	Angular momentum
h	Distance from the rear body (main frame) mass center to x-axis
h'	Distance from the mass center of the entire body to x-axis
h_R	Distance from the driver mass center to x-axis
I_{fs}, I_{ft}	Moments of inertia of the front fork with respect to xs-axis and xt-axis
I_{rx}, I_{rz}	Moments of inertia of the main frame with respect to x-axis and z-axis
I_{rxz}	Product of inertia of the main frame
i	Polar moment of inertia of the engine flywheel
i_{fx}, i_{fy}, i_{fz}	Moments of inertia of the front wheel with respect to x-axis, y-axis and z-axis
i_{m1x}, i_{m1z}	Rolling and yawing moments of inertia of the rider
i_{ry}	Moment of inertia of the rear wheel with respect to y-axis
j	Distance from the front fork center of mass to x-axis
k	Distance from front fork center of mass to z-axis
l_f	Distance from the front wheel to z-axis
l_r	Distance from the rear wheel to z-axis
l_R	Distance from the rider center of mass to z-axis
M_f, M_r	Masses of the front and main frames
m_1	Mass of the rider
R_f, R_r	Radii of the front wheel and rear wheel
W	Vehicle weight in kilograms
X	Longitudinal displacement of the motorcycle
Y	Lateral displacement of the motorcycle

Z	Vertical displacement of the motorcycle
Y_f, Y_r	Lateral forces acting on the front and rear tires, respectively
Z_f	Load acting on the front wheel
Z_r	Load acting on the rear wheel
ε	Caster angle
μ	Friction coefficient
η	Trail
λ	Gear ratio between the rear wheel and the engine flywheel
τ	Steering torque applied by the rider
τ_1	Rider body controlling torque
ϕ	Roll angle of the vehicle
ϕ_1	Leaning angle of the rider body
ψ	Yaw angle of vehicle
φ	Pitch angle of the vehicle
δ	Steering angle
ω_1	Natural frequency representing rigidity of the rider body
ζ_1	Damping ratio of the rider body

REFERENCES

1. Aoki, A., 1979, "Experimental Study on Motorcycle Steering Performance," *SAE paper No. 790265.*
2. Chang, H. J., 1992, "Handling Analysis of A Motorcycle-Trailer Vehicle," *Thesis*, Department of Power Mechanical Engineering, The National Tsing Hua University, Taiwan.
3. Forsythe, G. E., Malcolm, M. A., and Moler, C. B., 1997, *Computer Methods for Mathematical Computations*, Prentice-Hall International, Inc.
4. Happian-Smith, J., Macaulay, M. A., and Chinn, B. P., 1987, "Motorcycle Impact Simulation and Practical Verification," *Proceedings of the 11th International Technical Conference on Experimental Safety Vehicles*, Washington D.C., May 12~15.
5. Happian-Smith, J., Macaulay, M. A., and Chinn, B. P., 1990, "Computer Simulation of a Simple Motorcycle in Glancing Impacts with a Rigid Barrier," *SAE paper* No. 900754.
6. Katayama, T., Aoki, A., and Nishimi, T., 1988, "Control Behaviour of Motorcycle Riders," *Vehicle System Dynamics*, Vol. 17, pp. 211-229.
7. Knight, R. E., and Peterson, H., 1971, "Dynamics of Motorcycle Impact, Volume II: Digital Computer Simulation of Two-Dimensional Motion of Motorcycle and Dummy Rider," *Final Report DOT-HS-800-588.*
8. Legouis, T., Lanevill, A., Bourassa, P., and Payre, G., 1986, "Characterization of Dynamic Vehicle Stability Using Two Models of Human Pilot Behavior," *Vehicle System Dy-namics*, Vol. 15, No. 1, pp. 1-17.
9. Liu, T. S., and Chen, J. S., 1992, "Nonlinear Analysis of Stability for Motorcycle-Rider Systems," *International Journal of Vehicle Design*, Vol. 13, No. 3, pp. 276-294.
10. Lupker, H. A., de Coo, P. J. A., Nieboer, J. J., and Wismans, J., 1991, "Advances in MADYMO Crash Simulation," *SAE paper* No. 910879.
11. Lupker, H. A., and Koppens, W. P., 1992, "MADYMO Vehicle Dynamics Application," *Proceedings of the 3rd International MADYMO Users' Meeting*, Detroit.
12. Nieboer, J. J., Wismans, J., Versmissen, A. C. M., Van Slagmaat, M. T. P., Kurawaki, I., and Ohara, H., 1993, "Motorcycle Crash Test Modeling," *SAE Paper* No. 933133.
13. Rice, R. S., 1978, "Rider Skill Influences on Motorcycle Maneuvering," *SAE paper* No.780312.
14. Sharp, R.S., 1971, "The Stability and Control of Motorcycles," *Journal of Mechanical Engineering Science*, Vol. 13, No. 5, pp. 316-329.
15. Sporner, A., 1982, "Experimentelle und Mathematische Simulation von Motorradkollisionen im Vergleich zum realen Unfallgeschehen," *Dissertation*, Technischen Universitat Munchen.
16. TNO Road-Vehicle Research Institute, 1994, "Controlled Motorcycle," *MADYMO Application 3D*, Chapter 10.
17. Wang, M. C., 1997, "Motorcycle Kinematic Behavior after A Collision," *Master Thesis*, Department of Civil Engineering, Tamkang University, Taiwan.
18. Weir, D. H., and Zellner, J. W., 1978, "Lateral-Directional Motorcycle Dynamics and Rider Control," *SAE paper* No.780304.
19. Weir, D. H., 1972, "Motorcycle Handling Dynamics and Rider Control and the Effect of Design Configuration on Response and Performance," Ph.D. *Dissertation*, University of California at Los Angeles.
20. Woolley, R. L., Warner, C. Y., and Perl, T. R., 1986, "An Overview of Selected Computer Programs for Automotive Accident Reconstruction," *Transportation Research Record 1068*, pp. 18-33.
21. Yeh, E. C., and Chen, Y. L., 1990, "Handling Analysis of A Motorcycle with Added Cambering of The Front Frame," *Vehicle System Dynamics*, Vol. 19, No. 2, pp. 49-70.

Manuscript Received: July 11, 2001
Revision Received: Jan. 08, 2002
and Accepted: Feb. 11, 2002

八自由維度動力模式展現碰撞後之摩托車運動行為

張堂賢

國立台灣大學土木工程學系暨研究所

摘　要

推導一精準的受撞摩托車運動行爲是開發摩托車事故分析工具的先期工作。本文成功地推導一高自由度之受撞摩托車運動行爲模式。本研究依據所推導模式在受撞摩托車運動行爲模擬中展示有二十四項時間響應圖示，包括橫向縱向垂直之位移、速度和加速度，車輛前傾角側偏角滾搖角和騎士之滾搖、方向把手之旋角、速度和加速度等之變化。並有一箴平面圖可共顯現車輛的運動軌跡。本項模式之開發可以用於摩托車受碰撞後是否穩定或翻覆之初步分析。

關鍵詞：兩輪車輛動力學，受撞摩托車之運動，事故分析工具。